

# RSC Advances

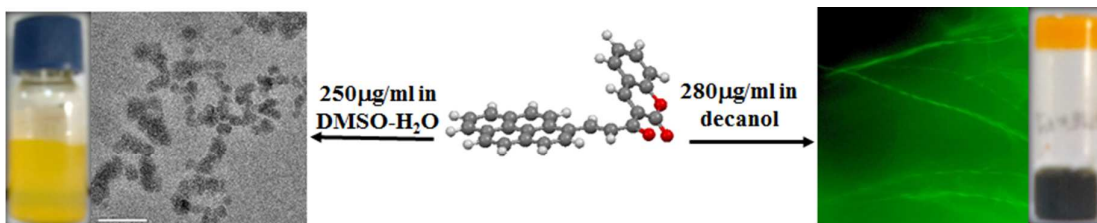


This is an *Accepted Manuscript*, which has been through the Royal Society of Chemistry peer review process and has been accepted for publication.

*Accepted Manuscripts* are published online shortly after acceptance, before technical editing, formatting and proof reading. Using this free service, authors can make their results available to the community, in citable form, before we publish the edited article. This *Accepted Manuscript* will be replaced by the edited, formatted and paginated article as soon as this is available.

You can find more information about *Accepted Manuscripts* in the [Information for Authors](#).

Please note that technical editing may introduce minor changes to the text and/or graphics, which may alter content. The journal's standard [Terms & Conditions](#) and the [Ethical guidelines](#) still apply. In no event shall the Royal Society of Chemistry be held responsible for any errors or omissions in this *Accepted Manuscript* or any consequences arising from the use of any information it contains.

**Abstract**

Multifunctional  $\pi$ -conjugated systems derived from renewable resource that self-assemble into supramolecular structures are reported. The aggregation of compounds in different solvents strongly influences its optical properties. These  $\pi$ -conjugated molecules can be used for live cell imaging applications. It also show low cytotoxicity in normal cells and suppresses the proliferation in PC3 prostate cancer cells.

Cite this: DOI: 10.1039/c0xx00000x

www.rsc.org/xxxxxx

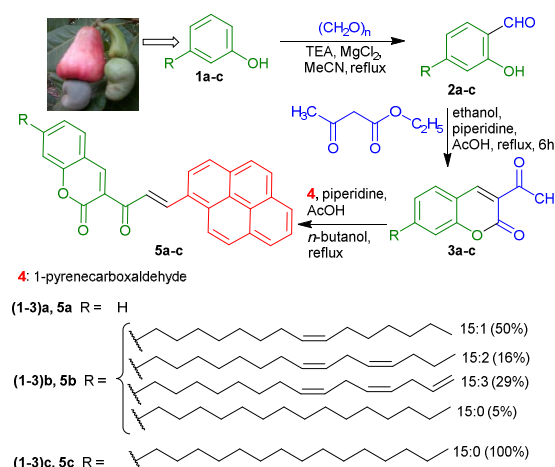
## ARTICLE TYPE

Self-assembled  $\pi$ -conjugated system as an anti-proliferative agent in prostate cancer cells and probe for intra-cellular imagingKrishnamoorthy Lalitha,<sup>a</sup> Preethi Jenifer,<sup>a</sup> Y. Siva Prasad,<sup>a</sup> Kumarasamy Muthusamy,<sup>a</sup> George John,<sup>b</sup> Subbiah Nagarajan,<sup>\*a</sup>Received (in XXX, XXX) Xth XXXXXXXXX 20XX, Accepted Xth XXXXXXXXX 20XX  
DOI: 10.1039/b000000x

Multifunctional  $\pi$ -conjugated systems derived from renewable resource that self-assemble into supramolecular structures are reported. The aggregation of compounds in different solvents strongly influences its optical properties. These  $\pi$ -conjugated molecules can be used for live cell imaging applications. It also show low cytotoxicity in fibroblast and suppresses the proliferation in PC3 prostate cancer cells.

The self-assembly of low molecular weight building blocks to form diverse supramolecular architectures has attracted substantial interest due to their versatile applications in the field of drug delivery, gene therapy, tissue engineering, enzyme immobilization, biosensors and construction of novel nano- or microscopic materials and devices.<sup>1-3</sup> In this context molecular gels are known as distinct class of soft materials. The gels are formed by the hierarchical assembly of low molecular weight organic gelators in a suitable solvent to structures such as fibrils, tapes, rods and tubes.<sup>4</sup> The specific non-covalent interactions such as hydrogen bonding,  $\pi$ - $\pi$  interaction, electrostatic and van der Waals interactions, hydrophilic-lipophilic balance (HLB) and other supramolecular weak forces are the driving forces for the self-assembly.<sup>5</sup> Fluorescent supramolecular gels derived from biologically relevant molecules have received much attention because of their wide range of applications. Coumarin, a class of naturally occurring benzopyrone derivative has been used as an important pharmacophore, as it displays biological activities such as anticancer, antibacterial, antifungal, anticoagulant and anti-HIV, to name a few.<sup>6</sup> The high fluorescence quantum yield and sensitivity toward the small changes in microenvironment are unique to the self-assembled pyrene derivatives, which enables them in applications in biomedical and biological research.<sup>7</sup> These prospects drive us through extensive synthetic efforts to obtain more diverse pyrene-coupled coumarin based  $\pi$ -gelator with various hydrophobic tails, which could be used as drug carrier under high concentration, cell imaging agent under lower concentration and may exhibit therapeutic value too. Organogels derived from " $\pi$ -gelators" are called " $\pi$ -gels" which are self-assembled soft materials obtained from gelators with more than one aromatic  $\pi$ -unit.<sup>7</sup> In the present studies,  $\pi$ -gelators were developed from renewable plant-derived resource, cashew nut shell liquid. Renewable resources have been used for several

decades, there has been considerable focus on establishing and optimizing efficient materials, biologically relevant molecules, and large-scale production of chemicals and fuels that address the needs of the 21<sup>st</sup> century.<sup>8</sup> Among the large number of renewable resources, cashew nutshell liquid (CNSL) is an important by-product obtained from the cashew nut industry.<sup>9</sup> The major component of CNSL being cardanol, a bio based non-isoprene lipid, comprising of rich mixture of phenolic lipids: 5% of 3-*n*-pentadecylphenol (3-PDP), 50% of 3-(8*Z*,11*Z*-pentadecenyl)phenol, 16% of 3-(8*Z*,11*Z*-pentadecadienyl)phenol and 29% of 3-(8*Z*,11*Z*,14-pentadecatrienyl)phenol. The naturally occurring varying degree of *cis*-double bonds and an odd number of carbon chain with easily accessible saturated and unsaturated hydrocarbon chains are the unique features of cardanol.<sup>9,10</sup> By harnessing electrophilic aromatic substitution reaction on phenol, we have synthesized both cardanol-aldehyde **2b** and PDP-aldehyde **2c**. The Knoevenagel reaction of compounds **2a-c** with ethyl acetoacetate under optimized reaction condition led to the desired 3-acetylcoumarins **3a-c** in good yields.<sup>11</sup>  $\pi$ -Gelators has been synthesized in good yields by aldol condensation of **3a-c** with 1-pyrenecarboxaldehyde **4** (Scheme 1).

Scheme 1. Synthesis of multifunctional coumarin-coupled pyrene derivatives **5a-c**.

Most of the pyrene based low molecular weight organogelator (LMOG) were prone to gelate solvents by using weak bonding mechanism in the presence of suitable solvents, even in the

absence of hydrogen bonding.<sup>12</sup> The supramolecular interaction of **5a** by means of  $\pi$ - $\pi$  stacking is inferred by NMR spectral analysis (Figure S1). Self-assembly of such an efficient gelator through non-covalent interactions into fibrillar aggregate that could immobilize the solvent molecule by capillary force to form a gel.<sup>4</sup> Gelation studies using aromatic solvents, alcohols and vegetable oils were carried out (Table S1).  $\pi$ -Gelators **5a** and **5b** exhibit excellent organogelation ability, showing critical gelation concentrations (CGCs) of 0.28 and 1.0 % (wt/v) respectively in higher alcohols such as decanol and dodecanol.  $\pi$ -Conjugated molecule **5c** did not form gel because of its enhanced hydrophobicity. Gel-Sol transition temperature ( $T_g$ ) was determined by typical test tube inversion method.<sup>4</sup> In fact organogel formed by these compounds experience a gel to sol transition upon heating-cooling cycles ( $T_g = 65^\circ\text{C}$ ). Morphology of the aggregates constitutive of the organogel in dodecanol has been identified using optical microscopy imaging deposited on glass slide. It shows thin fiber and twisted fiber-like structures of 100-200 nm thickness that bundle to form 3D network (Figure 1). Morphology and properties of the  $\pi$ -gel resembles the self-assembly mechanism of  $\pi$ -conjugated molecule.<sup>7</sup> Detailed gelation test indicated that compound **5a-5c** do not form gel in any of the aromatic solvents tested and form stable gel in long chain alcohols and vegetable oils. Increasing the lipophilicity of the coumarin coupled pyrene derivative by introducing unsaturated and saturated alkyl chain decreases the gelation ability. At lower concentration, **5a-c** in DMSO-water mixture ( $1 \times 10^{-3}\text{M}$  solution) form self-assembled nano-sheets and nano-flakes (Figure 1). Nanoparticle formation was further confirmed using particle size analyser (Zetasizer). The average sizes of self-assembled aggregates of **5a-c** in DMSO-water mixture ( $1 \times 10^{-3}\text{M}$  solution) are 194, 21 and 274 nm respectively (See ESI).

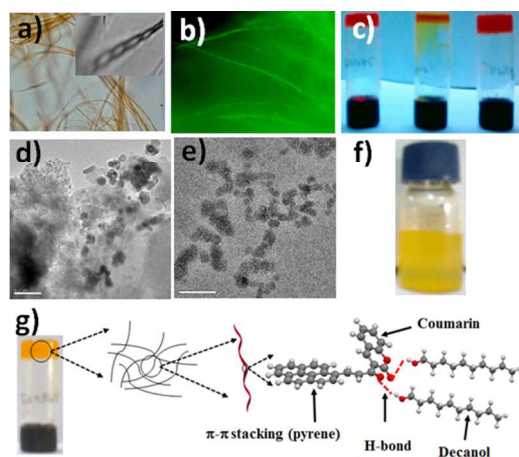


Figure 1. (a&b) Optical microscopy image of gel, **5a** in dodecanol (0.28 % wt/v) under white light and fluorescence light respectively, inset show the formation of twisted fibers; (c) Pictures of gel under UV light [left-**5a** in decanol, middle-**5b** in hazelnut oil and right-**5a** in dodecanol]; (d&e) HRTEM images of the self-assembly of **5a** and **5b** in DMSO-water mixture respectively; (f) Picture of self-assembled solution of **5a** in DMSO-water (1:1 ratio;  $1 \times 10^{-3}\text{M}$  solution) and (g) Schematic representation of gel formation.

Small-angle X-ray diffraction (SAXD) was employed to acquire an additional insight into the structures that constitute the gel formed from supergelator **5a**. XRD of the wet gel provides a Bragg's reflection at 1.35 nm, 1.30 nm, 1.26 nm which

enunciates coumarin coupled pyrene, intercalated free decanol and hydrogen bonded decanol with the carbonyl group of coumarin-coupled pyrene derivative (Figure S2). This reflection is approximately equal to the molecular length of **5a**, which was confirmed by molecular modelling studies using energy minimized calculations. Sharp peaks observed between 0.98-0.62 nm may arise from packing of dodecanol (both free and hydrogen bonded dodecanol) due to van der Waals interaction in gel network. The broad peak at  $25^\circ$  is assignable to the (001) aspect of  $\pi$ - $\pi$  stacking of pyrene units.<sup>13</sup>

The UV-vis spectrum of compound **5a** in acetonitrile shows three bands centred at 307, 392 and 427 nm, which are attributed to coumarin and pyrene unit under un-aggregated form. By changing the solvent to DMSO, the peak observed at 307 nm shifted to 352 nm and other peaks remained as same. This result implies the weak interaction of DMSO with coumarin core of **5a**. Compound **5a** in dodecanol show bands at 324 and 448 nm, red shift in all these peaks are due to molecular aggregation involving the formation of hydrogen bonding between carbonyl carbons of coumarin moiety and dodecanol, and  $\pi$ - $\pi$  stacking of pyrene (Figure 2a). Based on the results, we propose molecular arrangement of **5a** in higher alcohol (Figure 1).<sup>14</sup> The UV titration of compound **5a** dissolved in DMSO ( $1 \times 10^{-5}\text{M}$ ) with PBS buffer solution were then conducted. As expected, with the continuous addition of  $100\mu\text{L}$  of PBS buffer, absorbance band at 427 nm decreases with gradual increase in volume of PBS buffer solution. This property is attributed to the formation of nano-structures by self-assembly of pyrene and coumarin moieties (Figure 2b). After the investigation of the self-assembly features of **5a** in solution using UV-vis spectroscopy, we have evaluated the fluorescence property of **5a** in solution and self-assembled state. The intense fluorescence observed in the gel state stimulated us to explore the emission property of compound **5a-c** under different experimental conditions to confirm the influence of aggregation of the material. In self-assembled state, emission spectrum of **5a** in dodecanol shows three peaks at 389, 409 and 554, which on further titration using dodecanol, the intensity of peak observed at 409 nm got decreased and 554 nm show blue shift and is attributed to the disassembly behaviour of self-assembled pyrene moiety (Figure 2c). Similarly, compound **5a** in DMSO shows three intense peaks at 397, 409 and 478 nm (Figure S3). The molecular aggregation in supergelator **5a** dissolved in DMSO was induced by stepwise addition of  $100\mu\text{L}$  of PBS buffer and its emission behaviour was also followed. In the aggregated state, the emission spectrum covers a broad range of visible spectral range and exhibit vibronic coupling maximum at 414 and 576 nm. The drastic increase in emission intensity with a red shift in the aggregated state implies the formation of self-assembled structure (Figure 2).<sup>15</sup> We determined fluorescence quantum yields of **5a-c** in different solvents ( $1 \times 10^{-5}\text{M}$ ). Compound **5a-c** exhibited a very low fluorescence quantum yield ranging from 9-12 % in DMSO-PBS buffer (1:1 ratio), which could be due to the self-aggregation of molecules. By using DMSO alone as a solvent increase in quantum yields (73%) was observed.



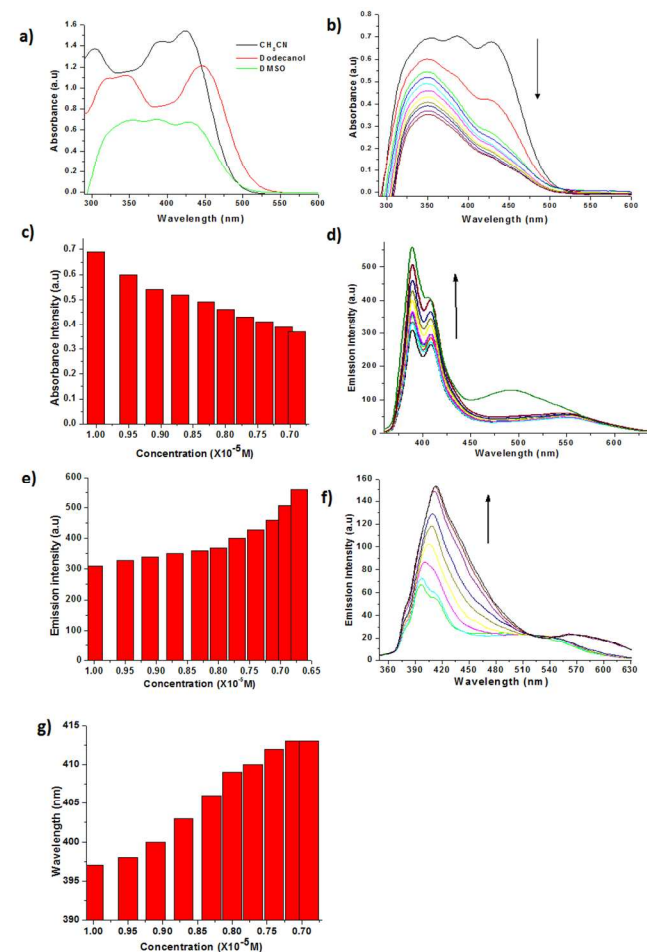


Figure 2. (a) UV-Vis spectra of **5a** in different solvents; (b & c) UV titration of **5a** in DMSO with PBS buffer and its corresponding plot of absorbance intensity vs concentration; (d) Emission spectra of **5a** in dodecanol ( $1 \times 10^{-5}$ ) and its response with respect to dilution [ $\lambda_{\text{ex}} = 325\text{nm}$ ]; (e) plot of emission intensity vs concentration of **5a** in dodecanol; (f & g) Fluorescence titration of **5a** in DMSO with PBS buffer [ $\lambda_{\text{ex}} = 325\text{nm}$ ] and its corresponding plot of wavelength vs concentration. In titration experiments, direction of arrow show the response of absorption and emission intensity with piecemeal addition of  $100\mu\text{L}$  of corresponding solvent.  $2\text{mL}$  of initial volume of solution ( $1 \times 10^{-5}$ ) was taken for titration experiments.

Similarly self-assembly of **5b** and **5c** was also identified by using UV and fluorescence studies (Figure S4 and S5). From these result, we resolve that at higher concentration, **5a** and **5b** form gel in decanol and dodecanol, and at lower concentration **5a-c** in DMSO-water (1:1 mixture) forms self-assembled nanostructures (nano-sheet and nano-flakes). Fluorescence of self-assembled system was not quenched even in extreme pH conditions (pH 4 & 10), and thus this system can be applied for cell imaging under physiologically important conditions at various pH values (Figure S6). In order to take the advantage of the utility of self-assembly of **5a-c** in DMSO-water mixture for live cell imaging application, normal (fibroblast) cells and PC3 human prostate cancer cells<sup>16</sup> were incubated with medium containing **5a-c** [**5a**:  $0.6 \times 10^{-3}\text{M}$ , **5b**:  $0.4 \times 10^{-3}\text{M}$  and **5c**:  $0.4 \times 10^{-3}\text{M}$  ( $250\mu\text{g}/1000\mu\text{L}$ )] for 24h and cellular localization was traced using Laser Confocal Scanning Microscopy (LCSM). Self-assembled coumarin-coupled pyrenes **5a-c** were uniformly located in the cytoplasm

and perinuclear region of the cells. The green self-fluorescence arising from **5a-c** can be readily observed. Fluorescence intensity decreases with increase in hydrophobicity of  $\pi$ -conjugated systems (Figure 3). Nanoparticles derived from **5a-c** were uniformly located into the cytoplasm of the cells. Endocytosis of nanoparticles involves four different mechanisms: Clathrin-mediated endocytosis, caveolae mediated endocytosis, macropinocytosis and phagocytosis. Inhibitors such as sucrose and chlorpromazine (blocking agents of clathrin-coated pit formation) and filipin (an inhibitor of caveolae-associated endocytosis) had no significant inhibition effect on the nanoparticle uptake. Nocodazole, an inhibitor of macropinocytosis decreases the uptake of nanoparticle up to 60%. The prominent cell uptake pathway for self-assembled nanoparticles are macropinocytosis and phagocytosis.<sup>16</sup> In fibroblast no damage in cells were observed, which implies the low cytotoxicity of fibroblast and also identified from cytotoxicity assay. In addition, the death of majority of PC3 cells were observed, which is due to anticancer activity of **5a-c**, as identified based on cell membrane rupture and the overflow of cytoplasm (Figure S7). Coumarin based anti-cancer drug, decursin inhibits Wnt/ $\beta$ -catenin pathway and cellular proliferation.<sup>17</sup> We hypothesize that **5a-c** might also follow similar of mechanism. This self-fluorescent probe would potentially facilitate a simultaneous combination of optical diagnosis and treatment for prostate cancer.

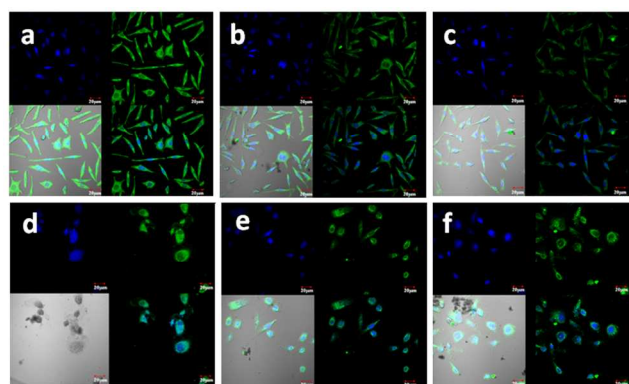


Figure 3. LCSM images of (a-c) fibroblast incubated with **5a-c** and (d-f) PC3 prostate cancer cells incubated with **5a-c** for 24h respectively. Green from self-fluorescent  $\pi$ -conjugated systems **5a-c** and blue from Hoechst stain used to differentiate nucleus.

In order to verify the biocompatibility of the fluorescent nanostructures, it is necessary to evaluate its *in vitro* cytotoxicity.<sup>18</sup> We have evaluated the cytotoxicity of compounds **5a-c** by MTS assay on fibroblast and PC-3 cells. The maximum absorbance ( $\lambda_{\text{abs}}$ ) of formazan, produced by the cleavage of MTS by dehydrogenases in living cells, at a wavelength of 490 nm is directly proportional to the number of live cells in the MTS assay. The  $\lambda_{\text{abs}}$  for compound **5a-c** in DMSO-water or DMSO-PBS buffer (1:1 mixture) was observed between 340-360nm, which would not interfere with MTS assay. Cytotoxicity assay shows that the fluorescent lipophilic compounds **5a-c** showed no significant cytotoxic effect on fibroblast. After 24h incubation, suppression in the proliferation of PC3 cells were observed and not in fibroblast. Inhibition in the proliferation of PC3 cells increases with increase in concentration of coumarin-coupled

pyrene derivatives **5a-c** (Figure S8).

In conclusion,  $\pi$ -conjugated systems derived from renewable resource that self-assemble into supramolecular structures through hydrogen bonding and  $\pi$ - $\pi$  stacking of pyrene units are reported. The aggregation of compounds in different solvents strongly influences its optical properties resulting in a redshift and increase of emission intensity. Under higher concentration, it form a gel and in lower concentration, self-assembled nanostructures was observed. Nanomaterial obtained under lower concentration were used for fibroblast and PC3 prostate cancer cell imaging applications. We hypothesise that suppression in the proliferation of PC3 cells might be due to the inhibition of Wnt/ $\beta$ -catenin pathway.<sup>17</sup> These self-assembled soft materials provide a promising platform for direct cell imaging and disease therapeutics. Further detailed investigation on mode of action is in progress in our research laboratory.

This work was financially supported by the Department of Science and Technology (IFA-CH-04 and #SB/FT/CS-024/2013), India and Board of Research in Nuclear Science (#37(1)/20/47/2014), Department of Atomic Energy, India. S.N thank DST, New Delhi for spectrofluorometer under the FIST sensor project scheme to SASTRA University. GJ acknowledges the support from the Gulf of Mexico Research Initiative (GoMRI) through the Consortium for the Molecular Engineering of Dispersant Systems (C-MEDS) subcontract (TUL-626-11/12). We also thank SASTRA University for TRR research fund.

## Notes and references

<sup>a</sup> Organic Synthesis Group, Department of Chemistry & The Centre for Nanotechnology and Advanced Biomaterials, School of Chemical and Biotechnology, SASTRA University, Thanjavur - 613401, Tamil Nadu, INDIA Fax: 04362264120; Tel: 04362304270; E-mail: nagarajan@scbt.sastra.edu.

<sup>b</sup> Department of Chemistry, the City College of New York, 160 Convent Ave. New York, NY 10031.

<sup>c</sup> We thank CARISM, SASTRA University for NMR facility.

† Electronic Supplementary Information (ESI) available: [Experimental details, figures, tables and copy of NMR spectra]. See DOI: 10.1039/b000000x/

- (a) D. Ma, K. Tu and L. M. Zhang, *Biomacromolecules* 2010, **11**, 2204; (b) Y. Qiu and K. Park, *Adv. Drug Delivery Rev.* 2001, **53**, 321; (c) K. Y. Lee and D. J. Mooney, *Chem. Rev.* 2001, **101**, 1869; (d) M. J. Wilson, S. J. Liliensiek, C. J. Murphy, W. L. Murphy and P. F. Nealey, *Soft Matter* 2012, **8**, 390; (e) V. Jayawarna, M. Ali, T. A. Jowitt, A. F. Miller, A. Saiani, J. E. Gough and R. V. Ulijn, *Adv. Mater.* 2006, **18**, 611.
- (a) B. D. MacCraith, C. M. McDonagh, G. O'Keeffe, A. K. McEvoy, T. Butler and F. R. Sheridan, *Sensors and Actuators B* 1995, **29**, 51; (b) J. Wang, *Anal. Chim. Acta* 1999, **399**, 21; (c) S. Banerjee, R. K. Das and U. Maitra, *J. Mater. Chem.* 2009, **19**, 6649; (d) A. Chakrabarty and U. Maitra, *J. Phys. Chem. B* 2013, **117**, 8039; (e) P. K. Vemula and G. John, *Chem. Commun.* 2006, 2218.
- (a) W. Jin and J. D. Brennan, *Anal. Chim. Acta* 2002, **461**, 1; (b) P. D. Thornton, R. J. Mart, S. J. Webb and R. V. Ulijn, *Soft Matter* 2008, **4**, 821; (c) M. Ghosh, S. Maiti, S. Brahmachari and P. K. Das, *RSC Adv.* 2012, **2**, 9042; (d) T. Kar, S. K. Mandal and P. K. Das, *Chem. Commun.* 2012, **48**, 8389; (e) B. Escuder, F. Rodriguez-Llansola and J. F. Miravet, *New J. Chem.* 2010, **34**, 1044; (f) Q. Wang, Z. Yang, X. Zhang, X. Xiao, C. K. Chang and B. Xu, *Angew. Chem. Int. Ed.* 2007, **46**, 4285; (g) N. M. Sangeetha and U. Maitra, *Chem. Soc. Rev.* 2005, **34**, 821; (h) S. Srinivasan, V. K. Praveen, R. Philip and A. Ajayaghosh, *Angew. Chem. Int. Ed.* 2008, **47**, 5675; (i) Y. Li, B. G. Cousins, R. V. Ulijn and I. A. Kinloch, *Langmuir* 2009, **25**, 11760; (j) A. M. Bieser and J. C. Tiller, *Supramol. Chem.* 2008, **20**, 363; (k) L. A. Estroff and A. D. Hamilton, *Angew. Chem. Int. Ed.* 2000, **39**, 3447; (l) S. Kiyonaka, K. Sada, I. Yoshimura, S. Shinkai, N. Kato and I. Hamachi, *Nat. Mater.* 2004, **3**, 58; (m) J. H. Jung, G. John, M. Masuda, K. Yoshida, S. Shinkai and T. Shimizu, *Langmuir* 2001, **17**, 7229; (n) S. Vauthey, S. Santoso, H. Y. Gong, N. Watson and S. G. Zhang, *Proc. Natl. Acad. Sci. USA* 2002, **99**, 5355; (o) P. K. Vemula, N. Wiradharma, J. A. Ankrum, O. R. Miranda, G. John and J. M. Krap, *Curr. Opin. Biotechnol.* 2013, **24**, 1; (p) M. Kumar, N. Kumar, V. Bhalla, P. R. Sharma and T. Kaur, *Org. Lett.*, 2012, **14**, 406; (q) B. Roy, P. Bairi and A. K. Nandi, *RSC Adv.*, 2014, **4**, 1708.
- R. G. Weiss and P. Terech, *Molecular Gels, Materials with Self-Assembled Fibrillar Networks*, Springer, New York, 2006.
- (a) S. Nagarajan, T. M. Das, P. Arjun and N. Raaman, *J. Mater. Chem.* 2009, **19**, 4587; (b) S. Nagarajan, P. Ravinder, V. Subramanian and T. M. Das, *New J. Chem.* 2010, **34**, 123; (c) G. John, B. Vijay Sankar, S. R. Jadhav and P. K. Vemula, *Langmuir* 2010, **26**, 17843; (d) G. John, M. Masuda, Y. Okada, K. Yase and T. Shimizu, *Adv. Mater.* 2001, **13**, 715.
- (a) T.-F. Yeh, C.-Y. Lin, and S.-T. Chang, *J. Agric. Food Chem.* 2014, **62**, 1706; (b) S. Robert, C. Bertolla, B. Masereel, J.-M. Dogne and L. Pochwet, *J. Med. Chem.* 2008, **51**, 3077; (c) A. Maresca, C. Temperini, L. Pochet, B. Masereel, A. Scozzafava and C. T. Supuran, *J. Med. Chem.* 2010, **53**, 335-344.
- S. S. Babu, V. K. Praveen, and A. Ajayaghosh, *Chem. Rev.* 2014, **114**, 1973 and reference cited therein.
- (a) L. K. Aggarwal, P. C. Thapliyal and S. R. Karade, *Progress in Organic Coatings*, 2007, **59**, 76; (b) T. Abhijit, J. Trissa and V. Vasant, *U. S. Pat. Appl. Publ.* 2012, US20120024527 A1 20120202; (c) A. L. M. Reddy, S. Nagarajan, P. Chumyim, S. R. Gowda, P. Pradhan, S. R. Jadhav, M. Dubey, G. John, and P. M. Ajayan, *Sci. Rep.* 2012, **2**, 960.
- (a) V. S. Balachandran, S. R. Jadhav, P. K. Vemula and G. John, *Chem. Soc. Rev.* 2013, **42**, 427; (b) H. S. P. Rao, M. Kamalraj, J. Swain and A. K. Mishra, *RSC Adv.* 2014, **4**, 12175; (c) B. Lochab, S. Shukla and I. K. Varma, *RSC Adv.*, 2014, **4**, 21712; (d) C. Voirin, S. Caillol, N. V. Sadavarte, B. V. Tawade, B. Boutevin and P. P. Wadgaonkar, *Polym. Chem.*, 2014, **5**, 3142; (e) W. Kiratitanavit, S. Ravichandran, Z. Xia, J. Kumar and R. Nagarajan, *J. Renew. Mater.* 2013, **1**, 289.
- (a) S. Kobayashi, H. Uyama and R. Ikeda, *Chem. Eur. J.* 2001, **7**, 4754; (b) L. Faure, S. Nagarajan, H. Hwang, C. L. Montgomery, B. R. Khan, G. John, P. Koulen, E. B. Blancaflor, and K. D. Chapman, *J. Biol. Chem.* 2014, **289**, 9340.
- J. Yao, W. Dou, W. Qin and W. Liu, *Inorg. Chem. Commun.* 2009, **12**, 116.
- (a) D. Mandal, T. Kar, and P. K. Das, *Chem. Eur. J.* 2014, **20**, 1349; (b) P. Xue, R. Lu, L. Zhao, D. Xu, X. Zhang, K. Li, Z. Song, X. Yang, M. Takafuji and H. Ihara, *Langmuir* 2010, **26**, 6669; (c) S. S. Babu, K. K. Kartha and A. Ajayaghosh, *J. Phys. Chem. Lett.* 2010, **1**, 3413; (d) F. Garcia, J. Buendía, S. Ghosh, A. Ajayaghosh and L. Sánchez, *Chem. Commun.* 2013, **49**, 9278; (e) K. Sakakibara, P. Chithra, B. Das, T. Mori, M. Akada, J. Labuta, T. Tsuruoka, S. Maji, S. Furumi, L. K. Shrestha, J. P. Hill, S. Acharya, K. Ariga and A. Ajayaghosh, *J. Am. Chem. Soc.* 2014, **136**, 8548.
- G. John, G. Zhu, J. Li and J. S. Dordick, *Angew. Chem. Int. Ed.* 2006, **45**, 4772.
- P. A. Korevaar, C. Schaefer, T. F. A. de Greef and E. W. Meijer, *J. Am. Chem. Soc.* 2012, **134**, 13482.
- (a) U. Rosch, S. Yao, R. Wortmann and F. Wurthner, *Angew. Chem., Int. Ed.* 2006, **45**, 7026; (b) A. Ajayaghosh, C. Vijayakumar, R. Varghese and S. George, *Angew. Chem., Int. Ed.* 2006, **45**, 456.
- (a) S. C. Lee, N. Y. Kang, S. J. Park, S. W. Yun, Y. Chandran and Y. T. Chang, *Chem. Commun.* 2012, **48**, 6681; (b) M. Vendrell, D. Zhai, J. C. Er and Y. T. Chang, *Chem. Rev.* 2012, **112**, 4491; (c) S. W. Yun, N. Y. Kang, S. J. Park, H. H. Ha, Y. K. Kim, J. S. Lee and Y. T. Chang, *Acc. Chem. Res.* 2014, **47**, 1277; (d) D. Zhai, W. Xu, L. Zhang and Y. T. Chang, *Chem. Soc. Rev.* 2014, **43**, 2402; (e) H. Gao, Z. yang, S. Zhang, S. Cao, S. Shen, Z. Pang, S. Jiang, *Sci. Rep.* 2013, **3**, 2534; (f) E. J. New, A. Congreve, D. parker, *Chem. Sci.* 2010, **1**, 111.

- 
17. G.-Y. Song, J.-H. Lee, M. Cho, B.-S. Park, D.-E. Kim and S. Oh, *Mol Pharmacol.* 2007, **72**, 1599.
  18. Y. Chen, P. A. Wilbon, J. Zhou, M. Nagarkatti, C. Wang, F. Chub and C. Tang, *Chem. Commun.* 2013, **49**, 297.

5